

# Superconductivity without attraction in a quasi-one-dimensional metal

A.V. Rozhkov

*Institute for Theoretical and Applied Electrodynamics RAS,  
Moscow, ul. Izhorskaya 13/19, 125412, Russian Federation*

(Dated: September 6, 2021)

An array of one-dimensional conductors coupled by transverse hopping and interaction is studied with the help of a variational wave function. This wave function is devised as to account for one-dimensional correlation effects. We show that under broad conditions our system possesses the superconducting ground state even if no attraction is present. The superconducting mechanism is of many-body nature and deviates substantially from BCS. The phase diagram of the model is mapped. It consists of two ordered phases competing against each other: density wave, spin or charge, and unconventional superconductivity. These phases are separated by the first order transition. The symmetry of the superconducting order parameter is a non-universal property. It depends on particulars of the Hamiltonian. Within the framework of our model possible choices are the triplet  $f$ -wave and the singlet  $d_{xy}$ -wave. Organic quasi-one-dimensional superconductors have similar phase diagram.

## I. INTRODUCTION

In this paper we will study a system of one-dimensional (1D) conductors arranged in a square lattice and coupled weakly in the transverse direction. The purpose of this work is to show that in a rather general situation such quasi-one-dimensional (Q1D) electron liquid with purely repulsive electron-electron interaction is either a superconductor, or an insulator with spin or charge density order. This is demonstrated with the help of a certain variational wave function which adequately captures 1D many-body effects.

The major issue in the description of the Q1D metal is the phenomenon of dimensional crossover. At high energy the system can be viewed as a collection of the Tomonaga-Luttinger (TL) liquids. However the TL liquid cannot support a physical electron as an elementary excitation. Thus, at low energy, where transverse single-electron hopping becomes important, it is necessary to abandon the TL notions and use the Fermi-liquid approach instead. Therefore, one is to stitch two different descriptions together to obtain complete picture.

From the technical point of view the source of the trouble is the conflict between the many-body TL correlations and transverse single-electron hopping, which is extremely difficult to handle within the framework of the 1D TL liquid [1].

A simple method for the crossover description was proposed in Ref.[2]. The latter method is based on a variational wave function, whose generalized version we will use in this paper.

To provide an intuitive introduction to the approach of [2] we briefly explain the structure of the variational wave function. Consider a 1D conductor described by the Tomonaga-Luttinger Hamiltonian. The ground state of this system is the ground state of all TL bosons, with every possible momenta  $k_{\parallel}$  ( $|k_{\parallel}| < \Lambda$ , where  $\Lambda$  is the cutoff

of the theory). Let's turn the transverse hopping on and couple  $N_{\perp}$  of these conductors into three-dimensional array. In this situation the system will attempt to lower its ground state energy even further by taking advantage of the transverse hopping energy. However, in order to participate in hopping the bosons have to form many-body fermion-like excitations, which have finite overlap with the physical fermion.

To accommodate for the possibility of having two types of excitations, bosonic and fermionic, we device our variational state in the following fashion. We introduce intermediate cutoff  $\tilde{\Lambda} < \Lambda$ . All TL bosons, whose energy and momenta are high ( $|k_{\parallel}| > \tilde{\Lambda}$ ), remain in their ground states. The small momenta bosons ( $|k_{\parallel}| < \tilde{\Lambda}$ ) form fermion-like excitations, which are delocalized in transverse direction. To distinguish between the physical electrons and these fermionic excitations we will refer to the latter as quasiparticles. In other words, the wave function can be factorized into two parts. The high-energy part corresponds to the ground state of  $|k_{\parallel}| > \tilde{\Lambda}$  Tomonaga-Luttinger bosons, the low-energy part corresponds to the three-dimensional anisotropic Fermi liquid composed of the quasiparticles.

The variational energy is minimized by adjusting  $\tilde{\Lambda}$ . The energy of the quasiparticle transverse hopping is decreasing function of  $\tilde{\Lambda}$ . At the same time, the in-chain energy grows when  $\tilde{\Lambda}$  grows. The trade-off between the transverse kinetic energy and the in-chain potential energy determines the value of  $\tilde{\Lambda}$ .

If the optimal value of  $\tilde{\Lambda}$  is non-zero, the low-energy excitations of the system are the quasiparticles. Properties of the fermionic quasiparticle state depend on quasiparticle effective Hamiltonian. It arises naturally after high-energy bosons are 'integrated out'. In this effective Hamiltonian the anisotropy is insignificant. Due to this circumstance, a standard mean field theory can be used to map out the quasiparticle phase diagram. Since the physical electron and the quasiparticle have finite overlap, there is a direct correspondence between broken symmetry phases of the effective Hamiltonian and the

physical system. We already mentioned that the possible phases of the system are spin-density wave (SDW), charge-density wave (CDW), and superconductivity. The mean-field treatment of the effective Hamiltonian was used in Ref. [3] in order to demonstrate the stability of the superconductivity in Q1D metals.

It is remarkable that the superconductivity is stable in the system with no attraction. Superconductivity cannot be found if one apply mean-field approximation to the bare Hamiltonian. To discover the existence of the superconducting ground state the high-energy degrees of freedom must be properly accounted for.

Our mechanism is related to that of Kohn and Luttinger. It is known that classical Kohn-Luttinger mechanism gives extremely low transition temperature. Our system does not share this property. Due to Q1D nature of the system the superconducting coupling constant is not as minuscule as Kohn-Luttinger coupling constant. Consequently, the transition temperature in our model does not have to be unobservable small.

We will see that the phase diagram of our model is similar to the phase diagram of the organic superconductors: (i) when the nesting of the Fermi surface is good, the ground state is either SDW or CDW; (ii) under increased pressure the nesting is spoiled, the density wave becomes unstable, and it is replaced by the unconventional superconductivity; (iii) under even higher pressure the superconducting transition temperature vanishes, and the system shows no sign of the spontaneous symmetry breaking. This similarity suggests that the proposed mechanism may be relevant for these materials.

Yet, the purpose of this paper is not to model real-life systems. Indeed, assumptions made about Hamiltonian's parameters may be too extreme for a real material. Rather, we want to demonstrate in a controllable way that the superconductivity in Q1D metals is a rather generic phenomena. Once this is done, the qualitative understanding developed in a specialized model may be applied to a more complicated situation, where analytical treatment is problematic.

The paper is organized as follows. In Sect. II we formulate our model. In Sect. III we perform its mean-field analysis. The variational calculations are done in Sect. IV. Different phases of the effective Hamiltonian (and the physical system) are mapped in Sect. V. We discuss the derived results in Sect. VI.

## II. THE SYSTEM

### A. The Hamiltonian

We start our presentation by writing down the Hamiltonian for the array of coupled 1D conductors:

$$H = \int_0^L dx \mathcal{H}, \quad (1)$$

$$\mathcal{H} = \sum_i \mathcal{H}_i^{1D} + \sum_{i,j} \left[ \mathcal{H}_{ij}^{\text{hop}} + \mathcal{H}_{ij}^{\rho\rho} \right], \quad (2)$$

where the indices  $i, j$  run over 1D conductors. In this paper we will adhere to the agreement of denoting the Hamiltonian densities with the calligraphic letters (e.g.,  $\mathcal{H}$ ) and full Hamiltonians with the italic letters (e.g.,  $H$ ).

In the above formula the Hamiltonian density  $\mathcal{H}_i^{1D}$  contains the in-chain kinetic energy and interactions:

$$\mathcal{H}_i^{1D} = \mathcal{T}_i^{1D} [\psi^\dagger, \psi] + \mathcal{V}_i^{1D} [\psi^\dagger, \psi] + \mathcal{V}_{\text{bs},i}^{1D} [\psi^\dagger, \psi], \quad (3)$$

$$\mathcal{T}_i^{1D} = -iv_F \sum_{p\sigma} p: \psi_{p\sigma i}^\dagger (\nabla \psi_{p\sigma i}):, \quad (4)$$

$$\mathcal{V}_i^{1D} = g_2 \sum_{\sigma\sigma'} \rho_{L\sigma i} \rho_{R\sigma' i} + g_4 (\rho_{L\uparrow i} \rho_{L\downarrow i} + \rho_{R\uparrow i} \rho_{R\downarrow i}), \quad (5)$$

$$\mathcal{V}_{\text{bs},i}^{1D} = g_{\text{bs}} \rho_{2k_F i} \rho_{-2k_F i}, \quad (6)$$

where the chirality index  $p$  is equal to  $+1$  ( $p = -1$ ) for right-moving (left-moving) electrons. The subscript 'bs' stands for 'backscattering'. The theory has an ultraviolet cutoff  $\Lambda = \pi/a$ . The symbol  $:\dots:$  denotes the normal order of the fermionic fields with respect to the non-interacting ground state. The Hamiltonian density  $\mathcal{H}_i^{1D}$  is spin-rotationally invariant.

Different densities used in formulae above and throughout the paper are defined by the equations:

$$\rho_{p\sigma i} = : \psi_{p\sigma i}^\dagger \psi_{p\sigma i} :, \quad (7)$$

$$\rho_i = \sum_{p\sigma} \rho_{p\sigma i}, \quad (8)$$

$$\rho_{2k_F i} = \sum_{\sigma} \psi_{R\sigma i}^\dagger \psi_{L\sigma i}, \quad (9)$$

$$\rho_{-2k_F i} = \rho_{2k_F i}^\dagger, \quad (10)$$

$$\mathbf{S}_{2k_F i} = \sum_{\sigma\sigma'} \vec{\tau}_{\sigma\sigma'} \psi_{R\sigma i}^\dagger \psi_{L\sigma' i}, \quad (11)$$

$$\mathbf{S}_{-2k_F i} = \mathbf{S}_{2k_F i}^\dagger, \quad (12)$$

where  $\vec{\tau}$  is the vector composed of the three Pauli matrices.

The coupling between the 1D conductors is described by the transverse terms: the single-electron hopping,

$$\mathcal{H}_{ij}^{\text{hop}} = -t(i-j) \sum_{p\sigma} \left( \psi_{p\sigma i}^\dagger \psi_{p\sigma j} + \text{H.c.} \right), \quad (13)$$

and the density-density interaction,

$$\mathcal{H}_{ij}^{\rho\rho} = g_0^\perp (i-j) \rho_i \rho_j + g_{2k_F}^\perp (i-j) (\rho_{2k_F i} \rho_{-2k_F j} + \text{H.c.}). \quad (14)$$

We accept that all interactions are repulsive, weak, and that the in-chain interactions are stronger than the transverse interactions:

$$2\pi v_F \gg g_{2,4} \gg g_{\text{bs}} \gg g_0^\perp \gtrsim g_{2k_F}^\perp > 0, \quad (15)$$

and the transverse hopping is small:

$$v_F \Lambda \gg t. \quad (16)$$

The constraints on the Hamiltonian's coefficients will be further discussed in Sect. IV, Sect. VB, and Sect. VIA.

### B. Bosonized Hamiltonian

In Sect. IV we will need the bosonized version of Hamiltonian density  $\mathcal{H}^{1D}$ . The bosonic representation is based on the bosonization prescription for the electron field [1]:

$$\psi_{p\sigma}^\dagger(x) = (2\pi a)^{-1/2} \eta_{p\sigma} e^{i\sqrt{2\pi}\varphi_{p\sigma}(x)}, \quad (17)$$

$$\varphi_{p\sigma} = \frac{1}{2} (\Theta_c + p\Phi_c + \sigma\Theta_s + p\sigma\Phi_s). \quad (18)$$

In the above formulae  $\eta_{p\sigma}$  is Klein factor,  $\Theta_{c,s}$  are the TL charge ( $c$ ) and spin ( $s$ ) boson fields,  $\Phi_{c,s}$  are the dual fields. The chain indices  $i, j$  are omitted in the expressions above. We will not show these indices explicitly in cases where such omissions do not introduce problems.

The bosonized one-chain Hamiltonian is:

$$\mathcal{H}^{1D}[\Theta, \Phi] = \mathcal{H}_0^{1D}[\Theta, \Phi] + \mathcal{V}_{bs}^{1D}[\Theta, \Phi], \quad (19)$$

where  $\mathcal{H}_0^{1D}$  is quadratic in the boson fields:

$$\begin{aligned} \mathcal{H}_0^{1D}[\Theta, \Phi] &= \mathcal{T}^{1D}[\Theta, \Phi] + \mathcal{V}^{1D}[\Theta, \Phi] \\ &= \frac{v_c}{2} \left( \mathcal{K}_c : (\nabla\Theta_c)^2 : + \mathcal{K}_c^{-1} : (\nabla\Phi_c)^2 : \right) \\ &\quad + \frac{v_s}{2} \left( : (\nabla\Theta_s)^2 : + : (\nabla\Phi_s)^2 : \right), \end{aligned} \quad (20)$$

while  $\mathcal{V}_{bs}^{1D}$  is not:

$$\begin{aligned} \mathcal{V}_{bs}^{1D}[\Theta, \Phi] &= \frac{g_{bs}}{2\pi^2 a^2} \cos(\sqrt{8\pi}\Phi_s) \\ &\quad - \frac{g_{bs}}{2\pi} \left[ : (\nabla\Phi_c)^2 : + : (\nabla\Phi_s)^2 : \right]. \end{aligned} \quad (21)$$

The symbol  $\dots$  denotes normal ordering of TL boson operators with respect to the non-interacting ( $\mathcal{K}_c = 1$ ,  $v_s = v_c$ ,  $g_{bs} = 0$ ) bosonic ground state. The Tomonaga-Luttinger liquid parameters are given by the formulae:

$$\mathcal{K}_c = \sqrt{\frac{2\pi v_F + g_4 - 2g_2}{2\pi v_F + g_4 + 2g_2}}, \quad (22)$$

$$v_c = \frac{1}{2\pi} \sqrt{(2\pi v_F + g_4)^2 - 4g_2^2}, \quad (23)$$

$$v_s = v_F - \frac{g_4}{2\pi}. \quad (24)$$

It is worth noting that

$$\mathcal{K}_c < 1, \quad (25)$$

for repulsive interaction.

We will also need the expression:

$$\psi_{R\sigma}^\dagger \psi_{L\sigma} = \frac{1}{2\pi a} e^{i\sqrt{2\pi}(\Phi_c + \sigma\Phi_s)}, \quad (26)$$

which gives operator  $\psi_{R\sigma}^\dagger \psi_{L\sigma}$  in terms of the TL bosons.

## III. THE MEAN-FIELD APPROACH

Once the model is formulated, it is not difficult to analyze its mean-field phase diagram. Such analysis introduces serious qualitative errors. Yet, in order to appreciate fully the advantage of the many-body calculations proposed below the comparison with the mean-field results is very important.

From the outset we have to keep in mind that in our system several different symmetries might be broken. Thus, several order parameters should be taken into consideration: SDW, CDW, triplet and singlet superconductivity.

To perform the mean-field analysis we write the interaction terms as products of these order parameters. After that the order corresponding to the highest coupling constant and susceptibility is chosen.

### A. CDW and SDW

We start with the in-chain interaction (the biggest potential energy in the system):

$$\begin{aligned} \mathcal{V}_i^{1D} + \mathcal{V}_{bs,i}^{1D} &= - \left( \frac{g_2}{2} - g_{bs} \right) \rho_{2k_F i} \rho_{-2k_F i} \\ &\quad - \frac{g_2}{2} \mathbf{S}_{2k_F i} \cdot \mathbf{S}_{-2k_F i} + \dots, \end{aligned} \quad (27)$$

where  $\dots$  stand for  $g_4$  term, which cannot be written as a product of two order parameters.

The transverse Hamiltonian may be expressed as a product of CDW and SDW order parameters:

$$\begin{aligned} \sum_{ij} \mathcal{H}_{ij}^{\rho\rho} &= \sum_{ij} g_{2k_F}^\perp (\rho_{2k_F i} \rho_{-2k_F j} + \text{H.c.}) \\ &\quad - g_0^\perp (\rho_{2k_F ij} \rho_{-2k_F ij} + \mathbf{S}_{2k_F ij} \cdot \mathbf{S}_{-2k_F ij}) + \dots \end{aligned} \quad (28)$$

The order parameter  $\rho_{2k_F ij}$  is equal to  $\sum_\sigma \psi_{R\sigma i}^\dagger \psi_{L\sigma j}$ , and  $\mathbf{S}_{2k_F ij}$  is defined in a similar fashion. They are bond CDW and bond SDW. These types of order cannot take advantage of the in-chain interaction energy (the biggest interaction energy in the problem). Thus, they cannot compete against  $\rho_{2k_F i}$  and  $\mathbf{S}_{2k_F i}$ . We will not study  $\rho_{2k_F ij}$  and  $\mathbf{S}_{2k_F ij}$  anymore.

The non-interacting susceptibilities of SDW and CDW are equal to each other. Eqs. (27) and (15) suggest that the SDW coupling constant is bigger than the CDW coupling constant:

$$g_{SDW} = \frac{g_2}{2} > g_{CDW} = \frac{g_2}{2} - g_{bs} + \frac{z^\perp g_{2k_F}^\perp}{2}, \quad (29)$$

where  $z^\perp$  is the number of the nearest neighbours of a given chain. Thus, when the nesting is good, the mean-field analysis suggests that the ground state is SDW.

## B. Superconducting orders

Several sorts of the superconducting order parameter can be defined. They can be classified according to their spin and orbital symmetry. It is useful to define a  $2 \times 2$  matrix  $\hat{\Delta}_{ij}$  with components:

$$(\hat{\Delta}_{ij})_{\sigma\sigma'} = \psi_{L\sigma i}^\dagger \psi_{R\sigma' j}^\dagger, \quad (30)$$

and write  $\hat{\Delta}_{ij}$  as a sum of three symmetric matrices  $i\vec{\tau}\tau^y$  and one antisymmetric matrix  $i\tau^y$ :

$$\hat{\Delta}_{ij} = \frac{1}{\sqrt{2}} [\mathbf{d}_{ij} \cdot (i\vec{\tau}\tau^y) + \Delta_{ij} i\tau^y]. \quad (31)$$

The operator  $\Delta_{ij}(\mathbf{d}_{ij})$  is the singlet (triplet) order parameter corresponding to a Cooper pair composed of two electrons one of which is on chain  $i$  and the other is on chain  $j$ .

Furthermore,  $\hat{\Delta}_{ij}$  may be symmetrized with respect to the chain indices as well:

$$\hat{\Delta}_{ij}^{s/a} = \frac{1}{2} (\hat{\Delta}_{ij} \pm \hat{\Delta}_{ji}). \quad (32)$$

The superscript ‘s’ (‘a’) stands for ‘symmetric’ (‘antisymmetric’).

The operators  $\Delta_{ij}^{s/a}$  and  $\mathbf{d}_{ij}^{s/a}$  are defined in the same fashion. If  $i = j$ , the antisymmetric quantities are, obviously, zero.

As the following derivations show, all these variants of superconductivity are unstable at the mean-field level. The in-chain interaction energy can be expressed as:

$$\begin{aligned} \mathcal{V}_i^{1D} + \mathcal{V}_{bs,i}^{1D} &= (g_2 - g_{bs}) \mathbf{d}_{ii} \cdot \mathbf{d}_{ii}^\dagger \\ &+ (g_2 + g_{bs}) \Delta_{ii} \Delta_{ii}^\dagger + \dots \end{aligned} \quad (33)$$

For realistic interaction  $g_2 > g_{bs}$ . Therefore, the one-chain order parameters  $\mathbf{d}_{ii}$ ,  $\Delta_{ii}$  are unstable.

The inter-chain interaction can be written as a bilinear of the superconducting order parameters  $\mathbf{d}_{ij}^{s/a}$ ,  $\Delta_{ij}^{s/a}$ ,  $i \neq j$ :

$$\begin{aligned} \sum_{ij} \mathcal{H}_{ij}^{pp} &= \\ &\sum_{ij} 2(g_0^\perp - g_{2k_F}^\perp) [\Delta_{ij}^a (\Delta_{ij}^a)^\dagger + \mathbf{d}_{ij}^s \cdot (\mathbf{d}_{ij}^s)^\dagger] \\ &+ 2(g_0^\perp + g_{2k_F}^\perp) [\Delta_{ij}^s (\Delta_{ij}^s)^\dagger + \mathbf{d}_{ij}^a \cdot (\mathbf{d}_{ij}^a)^\dagger] + \dots \end{aligned} \quad (34)$$

For a realistic choice of the interaction constants:

$$g_{2k_F}^\perp < g_0^\perp. \quad (35)$$

Consequently, the two-chain order parameters are unstable, as well as their one-chain counterparts.

## C. Mean-field phase diagram

As a result of the above considerations the following mean-field phase diagram has emerged. If the nesting is good, the stable phase is SDW. It is characterized by the non-zero  $\langle \mathbf{S}_{2k_F i} \rangle$ . The SDW state competes with the CDW state (non-zero  $\langle \rho_{2k_F i} \rangle$ ). SDW wins for it does not frustrate the backscattering interactions while CDW does [see Eq.(27)].

In a system with poor nesting SDW becomes unstable [4]. The mean-field theory predicts that such systems have no spontaneously broken symmetry.

This phase diagram will be corrected in a qualitative manner when the cooperative effects are accounted for. We will show that the many-body phenomena force the violation of Eq.(35), which makes the superconductivity stable in the systems with poor nesting. The same phenomena may lead to violation of inequality (29), inducing transition into CDW rather than SDW.

## IV. VARIATIONAL PROCEDURE

In this section we develop the variational approach overcoming the deficiencies of the mean-field approximation.

To keep our discussion short, transparent, and intuitive we will assume that both backscattering and transverse interactions are zero:  $g_{bs} = 0$ ,  $g_{0,2k_F}^\perp = 0$ . In such a situation the Hamiltonian is equal to:

$$H' = \sum_i H_{0i}^{1D} + \sum_{ij} H_{ij}^{\text{hop}}. \quad (36)$$

The first part of  $H'$ , the one-chain Hamiltonian  $H_{0i}^{1D}$ , is quadratic in terms of the TL bosons. The second part of  $H'$ , the transverse hopping  $H^{\text{hop}}$ , is quadratic in terms of the physical fermion fields. Because of this circumstance, the variational derivations for  $H'$  are simpler than for generic  $H$ . Yet, such derivations retain the most important features of the general case. This makes  $H'$  an ideal object of initial investigation, which we extend later for the Hamiltonian with non-zero  $g_{bs}$  and  $g_{0,2k_F}^\perp$ .

Below the prime mark (') will be used to distinguish between the most general Hamiltonian  $H$ , Eq.(1), and the special case  $H'$ , Eq.(36). Likewise, the prime will decorate the objects associated with  $H'$  (e.g., effective Hamiltonian  $H^{\text{eff}'}$ , variational energy  $E^{V'}$ ).

We first explain the heuristic idea behind our variational wave function. Let us think of our system in terms of the TL bosons. The bosonized version of  $\mathcal{H}_0^{1D}$  is given by Eq. (19). However, the ground state  $|0_{1D}\rangle$  of  $H_0^{1D}$  is not a good approximation to the ground state of  $H'$  for the finite-order perturbation theory in  $t$  is not well-defined.

On the other hand, if we were to describe our system with the help of the bare electron degrees of freedom  $\psi$ ,  $\psi^\dagger$  we will not have problems to account for  $H^{\text{hop}}$ . But,

within the fermionic framework, the in-chain interaction energy is extremely difficult to handle.

To resolve this conflict we introduce the parameter  $\tilde{\Lambda} < \Lambda$  and separate the total phase space of the model into two parts, the low-energy part (the degrees of freedom whose energy is smaller than  $v_F \tilde{\Lambda}$ ) and the high-energy part (the degrees of freedom whose energy is higher than  $v_F \tilde{\Lambda}$ ) [2]. The high-energy part will be described in terms of the TL bosons, while the low-energy part will be described with the help of fermionic quasiparticles, which we will define below. The exact value of  $\tilde{\Lambda}$  is to be found variationally, as a trade-off between the in-chain interaction and the transverse hopping.

The formal implementation of this approach goes as follows. First, the TL boson fields are split into two components: fast (with large momentum  $k_{\parallel}$ :  $\Lambda > |k_{\parallel}| > \tilde{\Lambda}$ ) and slow (with small momentum  $k_{\parallel}$ :  $|k_{\parallel}| < \tilde{\Lambda}$ ). The fast (slow) component will be marked by ‘>’ (‘<’) superscript:

$$\Theta_{c,s}(x) = \Theta_{c,s}^{<}(x) + \Theta_{c,s}^{>}(x) \quad (37)$$

$$= \sum_{|k_{\parallel}| < \tilde{\Lambda}} \Theta_{c,s,k_{\parallel}} e^{ik_{\parallel}x} + \sum_{\tilde{\Lambda} < |k_{\parallel}| < \Lambda} \Theta_{c,s,k_{\parallel}} e^{ik_{\parallel}x},$$

$$\Phi_{c,s}(x) = \Phi_{c,s}^{<}(x) + \Phi_{c,s}^{>}(x) \quad (38)$$

$$= \sum_{|k_{\parallel}| < \tilde{\Lambda}} \Phi_{c,s,k_{\parallel}} e^{ik_{\parallel}x} + \sum_{\tilde{\Lambda} < |k_{\parallel}| < \Lambda} \Phi_{c,s,k_{\parallel}} e^{ik_{\parallel}x}.$$

This split of the bosonic degrees of freedom induces the split of the in-chain Hamiltonian density  $\mathcal{H}_0^{1D}$ :

$$\mathcal{H}_0^{1D}[\Theta, \Phi] = \mathcal{H}_0^{1D}[\Theta^{<}, \Phi^{<}] + \mathcal{H}_0^{1D}[\Theta^{>}, \Phi^{>}]. \quad (39)$$

That is, the Hamiltonian  $H_0^{1D}$ , Eq.(20), cleanly separates into two parts corresponding to fast and slow modes.

The quasiparticles  $\Psi_{p\sigma}^{\dagger}(x)$  are defined with the help of Eq.(17), in which  $a$  is substituted by  $\tilde{a} = \pi/\tilde{\Lambda}$  and the slow fields  $\Theta_{c,s}^{<}$ ,  $\Phi_{c,s}^{<}$  or  $\varphi_{p\sigma}^{<}$  are placed instead of the bare fields  $\Theta_{c,s}$ ,  $\Phi_{c,s}$  or  $\varphi_{p\sigma}$ :

$$\Psi_{p\sigma}^{\dagger}(x) = (2\pi\tilde{a})^{-1/2} \eta_{p\sigma} e^{i\sqrt{2\pi}\varphi_{p\sigma}^{<}(x)}. \quad (40)$$

Using the quasiparticle field  $\Psi_{p\sigma}$  we refermionize  $\mathcal{H}_0^{1D}[\Theta^{<}, \Phi^{<}]$ :

$$\mathcal{H}_0^{1D} = \mathcal{H}_0^{1D}[\Psi^{\dagger}, \Psi] + \mathcal{H}_0^{1D}[\Theta^{>}, \Phi^{>}], \quad (41)$$

$$\mathcal{H}_0^{1D}[\Psi^{\dagger}, \Psi] = \mathcal{T}^{1D}[\Psi^{\dagger}, \Psi] + \mathcal{V}^{1D}[\Psi^{\dagger}, \Psi], \quad (42)$$

where  $\mathcal{T}^{1D}[\Psi^{\dagger}, \Psi]$  and  $\mathcal{V}^{1D}[\Psi^{\dagger}, \Psi]$  are given by Eqs. (4) and (5).

The mixed representation of  $\mathcal{H}_0^{1D}$ , Eq.(41), makes no sense in pure 1D problems since  $\mathcal{H}_0^{1D}[\Psi^{\dagger}, \Psi]$  corresponds to an interacting 1D system, whose ground state and excitations have no simple representation in terms of  $\Psi$ 's. Indeed, our variational calculations will show that, if  $t = 0$ , then  $\tilde{\Lambda} = 0$ . That is, no room for the quasiparticles is left in 1D situation. However, if  $t \neq 0$ , the quasiparticles

delocalize in the transverse directions and lower the total energy of the system. In such a case  $\tilde{\Lambda}$  does not have to be zero, as we will demonstrate.

The Hamiltonian density  $\mathcal{H}^{\text{hop}}$  can be easily expressed within the framework of the mixed quasiparticle-fast boson representation. One observes that the physical fermion is simply:

$$\psi_{p\sigma}^{\dagger} = \sqrt{\tilde{a}/a} \Psi_{p\sigma}^{\dagger} e^{i\sqrt{2\pi}\varphi_{p\sigma}^{>}}, \quad (43)$$

and that the fermionic and bosonic parts in this definition commute with each other. Therefore:

$$\mathcal{H}_{ij}^{\text{hop}} = -\frac{\tilde{a}}{a} t \sum_{p\sigma} \Psi_{p\sigma i}^{\dagger} \Psi_{p\sigma j} e^{i\sqrt{2\pi}(\varphi_{p\sigma i}^{>} - \varphi_{p\sigma j}^{>})} + \text{H.c.} \quad (44)$$

Eqs. (41) and (44) determine the form of the total Hamiltonian  $H'$  in the mixed representation. Let us study this Hamiltonian.

The eigenenergies of the fast bosons are determined mostly by  $\mathcal{H}_0^{1D}[\Theta^{>}, \Phi^{>}]$ . These eigenenergies are bigger than  $\sim v_F \tilde{\Lambda}$ . Small hopping term is only a correction to this quantity. Thus, we simply neglect contribution of  $H^{\text{hop}}$  to the high-energy sector's properties and assume that all fast bosons are in the ground state  $|0_{>}\rangle$  of the quadratic Hamiltonian:

$$H^{>} = \sum_i \int \mathcal{H}_{0i}^{1D}[\Theta^{>}, \Phi^{>}] dx. \quad (45)$$

When describing the quasiparticle state, we cannot neglect  $\mathcal{H}^{\text{hop}}$ : the quasiparticles are low-lying excitations, and their energy may be arbitrary small. Thus, we construct our variational wave function as a product:

$$|\text{var}\rangle = |\{\Psi\}\rangle |0_{>}\rangle, \quad (46)$$

where  $|\{\Psi\}\rangle$  is the unknown quasiparticle state. The variational energy is given by:

$$E^{V'} = \langle \text{var} | H' | \text{var} \rangle = \langle \{\Psi\} | H^{\text{eff}'} | \{\Psi\} \rangle. \quad (47)$$

This equation defines the effective quasiparticle Hamiltonian  $H^{\text{eff}'}$  as a ‘partial average’ over the fast degrees of freedom:

$$\begin{aligned} H^{\text{eff}'} &= \langle 0_{>} | H' | 0_{>} \rangle \\ &= H_0^{1D}[\Psi^{\dagger}, \Psi] + \tilde{H}^{\text{hop}}[\Psi^{\dagger}, \Psi] + \langle 0_{>} | H^{>} | 0_{>} \rangle, \end{aligned} \quad (48)$$

where the last term is the  $c$ -number corresponding to the fast boson contribution to the variational energy, and the effective quasiparticle hopping in Eq.(48) is defined by the formula:

$$\tilde{\mathcal{H}}_{ij}^{\text{hop}} = -\tilde{t} \sum_{p\sigma} \Psi_{p\sigma i}^{\dagger} \Psi_{p\sigma j} + \text{H.c.}, \quad (49)$$

$$\tilde{t} = t \frac{\Lambda}{\tilde{\Lambda}} \langle e^{i\sqrt{2\pi}\varphi_{p\sigma}^{>}} \rangle_{>}^2. \quad (50)$$

The symbol  $\langle \dots \rangle_{>}$  is the short-hand notation for  $\langle 0_{>} | \dots | 0_{>} \rangle$ . The fast bosons introduce renormalization

of the effective hopping of the quasiparticles. The expectation value in Eq.(50) is:

$$\langle e^{i\sqrt{2\pi}\varphi_{p\sigma}^>} \rangle = \left( \frac{\tilde{\Lambda}}{\Lambda} \right)^{(\mathcal{K}_c + \mathcal{K}_c^{-1} + 2)/8}. \quad (51)$$

To establish the above equality we must remember that  $|0_{>}\rangle$  is the ground state of the quadratic Hamiltonian  $H^>$ . Thus:

$$\langle e^{i\sqrt{2\pi}\varphi_{p\sigma}^>} \rangle = e^{-\pi\langle(\varphi_{p\sigma}^>)^2\rangle}, \quad (52)$$

$$\langle(\varphi_{p\sigma}^>)^2\rangle = \quad (53)$$

$$\begin{aligned} & \frac{1}{4} [\langle(\Theta_c^>)^2\rangle + \langle(\Phi_c^>)^2\rangle + \langle(\Theta_s^>)^2\rangle + \langle(\Phi_s^>)^2\rangle] \\ & = \frac{1}{8\pi} [\mathcal{K}_c^{-1} + \mathcal{K}_c + 2] \ln \frac{\tilde{\Lambda}}{\Lambda}. \end{aligned}$$

Substituting Eq.(51) into Eq.(50) one finds:

$$\tilde{t} = t \left( \frac{\tilde{\Lambda}}{\Lambda} \right)^{(\mathcal{K}_c + \mathcal{K}_c^{-1} - 2)/4}. \quad (54)$$

Assume now that the quasiparticle state  $|\{\Psi\}\rangle$  is non-interacting fermion ground state. Then the variational energy may be expressed as follows:

$$E^{V'}/LN_{\perp} = \varepsilon^{1D} + \varepsilon^F, \quad (55)$$

where  $L$  is the length of the sample along the 1D conductors,  $N_{\perp}$  is the number of these conductors; the one-dimensional contribution  $\varepsilon^{1D}$  and the non-interacting fermion contribution  $\varepsilon^F$  are equal to:

$$\varepsilon^{1D} = \frac{v_c\theta}{2\pi} (\tilde{\Lambda}^2 - \Lambda^2), \quad (56)$$

$$\varepsilon^F = -\frac{4}{\pi v_F} \sum_i [\tilde{t}(i)]^2 = -\frac{4}{\pi v_F} \left( \frac{\tilde{\Lambda}}{\Lambda} \right)^{2\theta} \sum_i [t(i)]^2, \quad (57)$$

$$\theta = \frac{1}{4} (\mathcal{K}_c + \mathcal{K}_c^{-1} - 2). \quad (58)$$

Our expression for the fermion energy neglects all corrections coming from quasiparticle interaction and possible symmetry breaking since these are small.

It is convenient to define the characteristic transverse hopping energy as:

$$\bar{t}^2 = \sum_i [t(i)]^2, \quad (59)$$

and the dimensionless ratio:

$$\zeta = \frac{\tilde{\Lambda}}{\Lambda} < 1. \quad (60)$$

In terms of such quantities the variational energy is equal to:

$$E^{V'}/LN_{\perp} = \frac{v_c\theta}{2\pi} \Lambda^2 (\zeta^2 - 1) - \frac{4}{\pi v_F} \zeta^{2\theta} \bar{t}^2. \quad (61)$$

Minimizing it with respect to  $\zeta$  one finds that for small in-chain interactions ( $\theta < 1$ ):

$$\zeta = \left( \frac{8\bar{t}^2}{v_c v_F \Lambda^2} \right)^{1/(2-2\theta)}. \quad (62)$$

We see that, if  $t = 0$ , the variational value of  $\tilde{\Lambda}$  is zero. In other words, in pure 1D system the quasiparticles do not appear.

Another important result obtained from Eq.(62) is:

$$\tilde{t} \sim v_F \tilde{\Lambda}. \quad (63)$$

This means that the anisotropy coefficient of the effective Hamiltonian is of order unity:  $(\tilde{t}/v_F \tilde{\Lambda}) \sim 1$ . Therefore, the mean-field treatment is appropriate for  $H^{\text{eff}'}$ . The latter conclusion is crucial for it signifies the completion of our quest: the microscopic Hamiltonian  $H'$ , Eq.(36), whose treatment is complicated by the presence of the 1D many-body effects, is replaced by the effective Hamiltonian  $H^{\text{eff}'}$ , Eq. (48), which can be studied with the help of the mundane mean-field approximation.

Finally, we must extend the derivation of the effective Hamiltonian to the situation of non-zero backscattering and transverse interactions. As with the case of  $H'$ , the effective Hamiltonian  $H^{\text{eff}}$  for the generic Hamiltonian  $H$  is defined by the equation  $H^{\text{eff}} = \langle H \rangle_{>}$ . It is straightforward to show that  $H^{\text{eff}}$  has the same form as  $H$  but with certain renormalizations of the coupling constants:

$$\tilde{g}_2 = g_2, \quad \tilde{g}_4 = g_4, \quad (64)$$

$$\tilde{g}_{\text{bs}} = g_{\text{bs}}, \quad \tilde{g}_0^{\perp} = g_0^{\perp}, \quad (65)$$

$$\tilde{t} = \zeta^{\theta} t, \quad \tilde{g}_{2k_F}^{\perp} = \zeta^{\mathcal{K}_c - 1} g_{2k_F}^{\perp}. \quad (66)$$

The derivations of these expressions are similar to the derivation of Eq.(54). For example, to calculate  $\tilde{g}_{2k_F}^{\perp}$  we must write:

$$\langle g_{2k_F}^{\perp} \rho_{2k_F i} \rho_{-2k_F j} \rangle_{>} \quad (67)$$

$$\begin{aligned} & = g_{2k_F}^{\perp} \left( \frac{\tilde{\Lambda}}{\Lambda} \right)^2 \sum_{\sigma\sigma'} \Psi_{R\sigma i}^{\dagger} \Psi_{L\sigma i} \Psi_{L\sigma' j}^{\dagger} \Psi_{R\sigma' j} \\ & \times \langle e^{i\sqrt{2\pi}[(\Phi_{ci}^> - \Phi_{cj}^>) + (\sigma\Phi_{si}^> - \sigma'\Phi_{sj}^>)]} \rangle_{>} \\ & = \tilde{g}_{2k_F}^{\perp} \sum_{\sigma\sigma'} \Psi_{R\sigma i}^{\dagger} \Psi_{L\sigma i} \Psi_{L\sigma' j}^{\dagger} \Psi_{R\sigma' j}, \end{aligned}$$

where the effective coupling constant  $\tilde{g}_{2k_F}^{\perp}$  is given by the expression:

$$\tilde{g}_{2k_F}^{\perp} = g_{2k_F}^{\perp} \left( \frac{\tilde{\Lambda}}{\Lambda} \right)^2 \langle e^{i\sqrt{2\pi}[(\Phi_{ci}^> - \Phi_{cj}^>) + (\sigma\Phi_{si}^> - \sigma'\Phi_{sj}^>)]} \rangle_{>}. \quad (68)$$

From this formula Eq.(66) for  $\tilde{g}_{2k_F}^{\perp}$  follows.

We want our effective Hamiltonian to be in the weak-coupling regime: when the coupling is weak, the kinetic energy of the quasiparticles dominates over their interaction, which justifies Eq.(57). Consequently, we need to

impose a restriction on magnitude of the effective coupling constants. Thus, in addition to Eq.(15) we require:

$$\tilde{g}_{2k_F}^\perp \ll 2\pi\tilde{v}_F. \quad (69)$$

Since  $\tilde{g}_{2k_F}^\perp = g_{2k_F}^\perp \zeta^{\mathcal{K}_c - 1}$ , inequality (69) is equivalent to:

$$\frac{\tilde{t}}{v_F \Lambda} \gg \left( \frac{g_{2k_F}^\perp}{v_F} \right)^{(1-\theta)/(1-\mathcal{K}_c)}. \quad (70)$$

This gives the lower bound on the transverse hopping. In Sect. VIA we will explain how this inequality should be modified in order to improve the accuracy of our method.

Keeping the above considerations in mind, one writes the equation for the effective Hamiltonian:

$$H^{\text{eff}} = H^{1D} + \tilde{H}^{\text{hop}} + \tilde{H}^{\rho\rho}, \quad (71)$$

where the tildes above  $\tilde{H}^{\text{hop}}$  and  $\tilde{H}^{\rho\rho}$  signify that the coupling constants of these terms are renormalized according to Eqs. (64), (65), and (66). The variational energy  $E^V$  and  $\zeta$  are given by Eqs.(55) and (62). The relation Eq.(63) holds true for Hamiltonian  $H^{\text{eff}}$  implying the applicability of the mean-field approximation.

Our variational derivation is equivalent to the tree-level renormalization group (RG) result. Namely, one can execute the following sequence of transformations. Beginning with the Hamiltonian  $H$  one bosonizes it to obtain the Tomonaga-Luttinger Hamiltonians for individual chains perturbed by the transverse interactions, transverse hopping, and in-chain backscattering. Because of the presence of relevant (in RG sense) operators the RG flow takes the Hamiltonian away from the Tomonaga-Luttinger fixed point. The flow must be stopped when the renormalized transverse hopping amplitude becomes of the order of the cutoff [see Eq.(63)]. At this point the bosonic Hamiltonian has to be refermionized. The resultant quasiparticle Hamiltonian coincides with  $H^{\text{eff}}$ . The relationship between the variational approach and the RG procedure is shown on Fig.1 in a form of a commutative diagram.

This completes our derivation of the effective quasiparticle Hamiltonian and we are prepared to analyze the phase diagram of our system.

## V. PHASE DIAGRAM

How the phase diagram of the Hamiltonian  $H$ , Eq.(1), can be determined? It is essential to realize that the phase diagram of  $H$  coincides with the phase diagram of  $H^{\text{eff}}$ . Consider, for example, the anomalous expectation value  $\langle \psi_{L\uparrow i}^\dagger \psi_{R\uparrow j}^\dagger \rangle$ . For such a quantity the following is correct:

$$\langle \psi_{L\uparrow i}^\dagger \psi_{R\uparrow j}^\dagger \rangle = \left( \frac{\Lambda}{\tilde{\Lambda}} \right) \langle \Psi_{L\uparrow i}^\dagger \Psi_{R\uparrow j}^\dagger \rangle \langle e^{i\sqrt{2\pi}\varphi_{p\sigma}^>} \rangle. \quad (72)$$

Since the bosonic expectation value is non-zero, both  $\langle \psi_{L\uparrow i}^\dagger \psi_{R\uparrow j}^\dagger \rangle$  and  $\langle \Psi_{L\uparrow i}^\dagger \Psi_{R\uparrow j}^\dagger \rangle$  are either simultaneously

zero or simultaneously non-zero. Same is true for other types of broken symmetries. This proves that the phase diagram of  $H$  and the phase diagram of  $H^{\text{eff}}$  are identical. Since the properties of  $H^{\text{eff}}$  are accessible through the mean-field approximation, we are fully equipped to explore the model's phase diagram.

### A. Density waves

First, we consider the density wave phases. Both SDW and CDW have the same susceptibilities but different effective coupling constants:

$$\tilde{g}_{\text{SDW}} = \frac{g_2}{2}, \quad (73)$$

$$\tilde{g}_{\text{CDW}} = \frac{g_2}{2} - g_{\text{bs}} + \frac{z^\perp \tilde{g}_{2k_F}^\perp}{2}. \quad (74)$$

Due to strong renormalization of  $\tilde{g}_{2k_F}^\perp$ , inequality Eq. (29), which is always satisfied for bare coupling constants, is not necessary fulfilled when the effective constants are compared. Therefore, depending on the microscopic details, the density wave phase could be of either nature. To be specific, we will study SDW below. The discussion for CDW is completely the same.

SDW in Q1D metal was thoroughly analyzed at the mean-field level in Ref. [4]. We will follow this reference.

As we know, the stability of SDW depends crucially on the nesting of the Fermi surface. Shape of the Fermi surface is determined by the effective transverse hopping amplitudes  $\tilde{t}(i)$ . If one assume that the only non-zero hopping amplitude is the nearest neighbor amplitude  $\tilde{t}_1$ , then the resultant Fermi surface nests perfectly. In order to describe the Fermi surface with non-ideal nesting it is necessary to include at least the next-to-nearest neighbor hopping amplitude  $\tilde{t}_2$ . For such structure of hopping the SDW susceptibility is equal to:

$$\chi_{\text{SDW}} \approx \frac{1}{\pi v_F} \times \begin{cases} \ln \left( 2v_F \tilde{\Lambda} / T \right), & \text{if } T > \tilde{t}_2 = \zeta^\theta t_2, \\ \ln \left( 2v_F \tilde{\Lambda} / \tilde{t}_2 \right), & \text{if } T < \tilde{t}_2 = \zeta^\theta t_2. \end{cases} \quad (75)$$

The SDW transition temperature is derived by equating  $(g_2/2)\chi_{\text{SDW}}$  and unity. For  $\tilde{t}_2 = 0$  it is:

$$T_{\text{SDW}}^{(0)} \propto v_F \tilde{\Lambda} \exp(-2\pi v_F / g_2). \quad (76)$$

If  $\tilde{t}_2 > 0$  the transition temperature  $T_{\text{SDW}}$  becomes smaller than  $T_{\text{SDW}}^{(0)}$ . It vanishes when  $\tilde{t}_2 \propto T_{\text{SDW}}^{(0)}$ . That is, exponentially small  $\tilde{t}_2$  is enough to destroy SDW.

### B. Superconductivity

The destruction of the density wave does not automatically implies that the ground state becomes superconducting. By analogy with Eq.(34) we can write for

the effective Hamiltonian:

$$\begin{aligned} \sum_{ij} \tilde{\mathcal{H}}_{ij}^{\rho\rho} = & \quad (77) \\ & \sum_{ij} 2(\tilde{g}_0^\perp - \tilde{g}_{2k_F}^\perp) \left[ \tilde{\Delta}_{ij}^a (\tilde{\Delta}_{ij}^a)^\dagger + \tilde{\mathbf{d}}_{ij}^s \cdot (\tilde{\mathbf{d}}_{ij}^s)^\dagger \right] \\ & + 2(\tilde{g}_0^\perp + \tilde{g}_{2k_F}^\perp) \left[ \tilde{\Delta}_{ij}^s (\tilde{\Delta}_{ij}^s)^\dagger + \tilde{\mathbf{d}}_{ij}^a \cdot (\tilde{\mathbf{d}}_{ij}^a)^\dagger \right] + \dots, \end{aligned}$$

where order parameters  $\tilde{\Delta}_{ij}^{s/a}$  and  $\mathbf{d}_{ij}^{s/a}$  are defined by Eqs.(30), (31), and (32), in which bare fermionic fields  $\psi$  and  $\psi^\dagger$  are replaced by the quasiparticle fields  $\Psi$  and  $\Psi^\dagger$ .

From Eq.(77) we see that the effective superconducting coupling constant  $\tilde{g}_{sc}$  is equal to:

$$\tilde{g}_{sc} = 2(\tilde{g}_{2k_F}^\perp - \tilde{g}_0^\perp). \quad (78)$$

We conclude that the superconductivity is stable if:

$$\tilde{g}_{2k_F}^\perp > \tilde{g}_0^\perp = g_0^\perp. \quad (79)$$

At the same time one has to remember that for the *bare* coupling constants the inequality  $g_{2k_F}^\perp < g_0^\perp$  holds true [see Eq.(35)]. Can both inequalities be satisfied at the same time? It is possible provided that the system is sufficiently anisotropic. Indeed, the inequalities (79) and (35) are equivalent to:

$$\frac{8\tilde{t}^2}{v_c v_F \Lambda^2} < \left( \frac{g_{2k_F}^\perp}{g_0^\perp} \right)^{(2-2\theta)/(1-\mathcal{K}_c)} < 1. \quad (80)$$

This is the necessary condition for the superconducting ground state. Similar condition was derived in [2] for the spinless electrons. This inequality gives an upper bound on  $t$ . This bound will be discussed in Sect. VIA in connection with the method's dependability.

The final question is the type of the superconducting order realized in our system. As one can see from Eq.(77) there are two candidates: singlet order parameter  $\Delta_{ij}^a$  ( $d_{xy}$ -wave according to the accepted naming scheme [5]) and triplet  $\mathbf{d}_{ij}^s$  ( $f$ -wave). Both have the same coupling constant of  $\tilde{g}_{sc}$ . This degeneracy cannot be lifted within our approach for we must include subtler effects into our consideration. We will argue below (Sect. VIB) that the answer is sensitive to microscopic details of the system. Therefore, in real materials either type of the superconductivity can be, in principle, realized.

### C. Global phase diagram

In this subsection we construct the global phase diagram of the system on the pressure-temperature plane.

The effect of the pressure on our Hamiltonian is twofold. First, it increases the next-to-nearest neighbor hopping amplitude  $t_2$ . Thus, the growth of the pressure spoils the nesting of the Fermi surface.

Second, it makes the system less anisotropic. This, in turn, leads to the reduction of the 1D renormalization of

$\tilde{g}_{2k_F}^\perp$  under increasing pressure. Therefore, one can say that  $\tilde{g}_{2k_F}^\perp$  is decreasing functions of pressure.

Consequently, at low pressure the nesting is good and the ground state is the density wave phase with the highest transition temperature possible:  $T_{SDW/CDW} = T_{SDW/CDW}^{(0)}$ . Under growing pressure the nesting property of the Fermi surface deteriorates and  $T_{SDW/CDW}$  becomes smaller.

The density wave transition temperature decays until some critical pressure  $p_c$  at which it quickly goes to zero. At  $p > p_c$  the subleading order, the superconductivity, is stabilized. The characteristic superconducting critical temperature is smaller than  $T_{SDW/CDW}^{(0)}$  for the density wave coupling constant is higher than that of the superconductivity. This is so because the density wave order benefits from the in-chain interaction  $g_{2\rho_L\rho_R}$  while the superconductivity cannot do this.

The superconducting order parameter is either triplet ( $f$ -wave) or singlet ( $d_{xy}$ -wave). The superconducting gap vanishes at four nodal lines on the Fermi surface.

Under even higher pressure  $T_c \rightarrow 0$  for the system becomes less anisotropic and inequality (79) becomes invalid.

The schematic diagram is shown on Fig.2.

## VI. DISCUSSION

This section is divided into four subsections. In subsection A we discuss the accuracy of our method.

In subsection B we speculate under what condition  $d_{x^2-y^2}$ -wave superconductivity may be stabilized.

In subsection C we compare our approach with other theoretical methods available in the literature.

In subsection D our theoretical results are compared against published experimental data.

In subsection E we give our conclusions.

### A. Accuracy of the variational approach

In general, variational approach is an uncontrollable approximation, and one may doubt our conclusions. Fortunately, the presented variational scheme is only a front for the tree-level RG transformation (see Fig. 1). Using RG notions, it is possible to prove rigorously that the superconductivity is stable at least in a certain parameter range. Since the stability of the superconducting phase depends on effective inter-chain interactions, we must show that the tree-level RG is enough to capture them adequately.

First, we must establish the structure of the tree-level RG flow. As implied by Eq.(15), our model is near the Tomonaga-Luttinger fixed point ( $g_{bs} = g_{0,2k_F}^\perp = 0$ ,  $t = 0$ ). The fixed point Hamiltonian is perturbed by two relevant operators,  $t$  and  $g_{2k_F}^\perp$ , and one marginal,  $g_{bs}$ .



We assume that the transverse hopping is the most relevant operator: at the dimensional crossover ( $\tilde{t} \sim v_F \tilde{\Lambda}$ ) inequality (69) is satisfied.

This tree-level picture disregards several corrections. The most well-known is  $(-g_{\text{bs}}^2)$  contribution to the RG equation for  $g_{\text{bs}}$ . This term is of little immediate interest to us since it does not affect the inter-chain interactions.

We identify three terms, which amend the RG equations for inter-chain interaction constants. First, the backscattering contributes to the anomalous dimension of  $g_{2k_F}^\perp$ : the term proportional to  $g_{\text{bs}} g_{2k_F}^\perp$  enters the RG equation for  $g_{2k_F}^\perp$ . This correction may be neglected since the anomalous dimension is proportional to  $g_2$ , which is much larger than  $g_{\text{bs}}$  [see (15)].

Second, the in-chain interactions combined with the transverse hopping contribute a term of order  $(g_{2,4}/v_F)^2 (t/v_F \Lambda)^2$ . This term corrects inter-chain couplings by the amount:

$$(\Delta g)_1 \sim \int_0^{\ell^*} d\ell \frac{[g_{2,4} t(\ell)]^2}{v_F^3 \Lambda^2(\ell)} \sim \frac{(g_{2,4})^2}{v_F}, \quad (81)$$

$$t(\ell) = t e^{-\theta \ell}, \quad (82)$$

where  $\ell$  denotes the scaling variable:  $\Lambda(\ell) = \Lambda e^{-\ell}$ . The dimensional crossover occurs, and our RG stops when  $\ell$  reaches the value  $\ell^* = \ln(\Lambda/\tilde{\Lambda})$ . At the crossover it is true:  $t(\ell^*)/[v_F(\ell^*)\Lambda(\ell^*)] = \tilde{t}/[v_F \tilde{\Lambda}] \sim 1$ .

Third, the inter-chain interactions may contribute to the scaling equations additional terms of order  $(g_{2k_F}^\perp)^2$ . Such term corrects inter-chain coupling constants by the amount:

$$(\Delta g)_2 \sim \int_0^{\ell^*} d\ell \frac{[g_{2k_F}^\perp(\ell)]^2}{v_F} \sim \frac{(\tilde{g}_{2k_F}^\perp)^2}{g_2}, \quad (83)$$

$$g_{2k_F}^\perp(\ell) = \tilde{g}_{2k_F}^\perp e^{-(1-\mathcal{K}_c)\ell}, \quad 1 - \mathcal{K}_c \sim g_2/v_F. \quad (84)$$

Thus, the corrections to  $\tilde{g}_{\text{sc}}$  beyond the tree-level may be disregarded if  $\tilde{g}_{2k_F}^\perp$  is much bigger than  $(\Delta g)_{1,2}$ . This condition is equivalent to:

$$(g_{2,4})^2/v_F \ll \tilde{g}_{2k_F}^\perp \ll g_2. \quad (85)$$

We already derived inequalities binding  $\tilde{g}_{2k_F}^\perp$  [see Eq.(69) and Eq.(79)]. Since  $v_F$  is bigger than  $g_2$ , Eq.(69) gives less restrictive upper bound on  $\tilde{g}_{2k_F}^\perp$  than Eq.(85). Therefore, if we want an assurance that our method does not lead us astray, we must abolish Eq.(69) and use Eq.(85) instead.

The situation with Eq.(79) is somewhat more complicated: it is impossible to know, which quantity,  $g_0^\perp$  or  $(g_{2,4})^2/v_F$ , is smaller. Thus, we define:

$$g_{\text{max}} = \max\{(g_{2,4})^2/v_F, g_0^\perp\}, \quad (86)$$

and rewrite Eq.(85) in the form:

$$g_{\text{max}} \ll \tilde{g}_{2k_F}^\perp \ll g_2. \quad (87)$$

This inequality is self-consistent in the sense that  $g_{\text{max}} \ll g_2$  [see Eq.(15)]. It is convenient to cast Eq. (87) and Eq.(16) as a constraint on the bare hopping amplitude:

$$\left(\frac{g_{2k_F}^\perp}{g_2}\right)^{\frac{1-\theta}{1-\mathcal{K}_c}} \ll \frac{t}{v_F \Lambda} \ll \left(\frac{g_{2k_F}^\perp}{g_{\text{max}}}\right)^{\frac{1-\theta}{1-\mathcal{K}_c}} \ll 1. \quad (88)$$

If this inequality is satisfied, then the model's phase diagram has a superconducting phase, and the superconductivity is not an artifact of the variational method. It is likely that some deviations from the constraints imposed by Eqs.(15) and (88) are not deadly for superconductivity. Yet, they may affect the order parameter symmetry. This issue is discussed in the next subsection.

## B. Symmetry of the superconducting order parameter

We have seen that the symmetry of the order parameter cannot be unambiguously determined within the framework of our approximation: as Eq.(77) suggests, both  $f$ -wave and  $d_{xy}$ -wave states have similar energies. Our method capture only gross features of the model, it is not delicate enough to calculate the superconducting coupling constant with higher accuracy. We can identify at least two mechanisms, which could lift the order parameter degeneracy. They work in opposite direction. Thus, the final outcome depends crucially on the minutiae of the microscopic model.

The mechanism promoting  $f$ -wave increases the coupling constant for this order parameter and decreases the  $d_{xy}$ -wave coupling constant. It operates in the following manner. The RG flow applied to our system generates a new spin-dependent transverse interaction:

$$\tilde{\mathcal{H}}_{ij}^{SS} = \tilde{J}_{2k_F}^\perp (i-j) \left( \tilde{\mathbf{S}}_{2k_F i} \cdot \tilde{\mathbf{S}}_{-2k_F j} + \text{H.c.} \right). \quad (89)$$

At the dimensional crossover ( $\tilde{t} \sim \tilde{v}_F \tilde{\Lambda}$ ) one has:  $\tilde{J}_{2k_F}^\perp \sim g_{2,4}^2/v_F$ . This estimate can be found in, e.g., Ref. [3] [see first row, second column of Table I where  $t'_\perp \sim E_0(l)$ ]. The new term can be cast as:

$$\sum_{ij} \tilde{\mathcal{H}}_{ij}^{SS} = \sum_{ij} -2\tilde{J}_{2k_F}^\perp \left[ \tilde{\mathbf{d}}_{ij}^s \cdot (\tilde{\mathbf{d}}_{ij}^s)^\dagger - 3\tilde{\Delta}_{ij}^a (\tilde{\Delta}_{ij}^a)^\dagger \right] + 2\tilde{J}_{2k_F}^\perp \left[ \tilde{\mathbf{d}}_{ij}^a \cdot (\tilde{\mathbf{d}}_{ij}^a)^\dagger - 3\tilde{\Delta}_{ij}^s (\tilde{\Delta}_{ij}^s)^\dagger \right]. \quad (90)$$

Thus, the  $f$ -wave coupling constant grows by  $2\tilde{J}_{2k_F}^\perp$ , and the  $d_{xy}$ -wave coupling constant decreases by  $6\tilde{J}_{2k_F}^\perp$ .

A factor in favor of the  $d_{xy}$ -wave superconductivity is the susceptibility. One can calculate two susceptibilities,  $\chi_f^{\text{sc}}$  and  $\chi_d^{\text{sc}}$ , for two order parameters:

$$\chi_{f,d}^{\text{sc}} = \frac{1}{2\pi v_F} \ln \left( \frac{\tilde{v}_F \tilde{\Lambda}}{T} \right) + C_{f,d}, \quad (91)$$

where  $C_{f,d}$  are the non-universal constants. In other words, the divergent parts of both susceptibilities are identical, but the non-singular parts depend on the order parameter symmetry and the band structure. This happens because our two orders have different orbital structure ( $f$ -wave is symmetric with respect to inversion of the transverse coordinate, while  $d_{xy}$ -wave is antisymmetric).

Within the framework of our model (linear dispersion along the  $x$ -axis, square lattice, small  $\tilde{t}_2$ ) we have  $C_f < C_d$ . Thus, the susceptibility of  $d$ -wave is higher.

The above analysis demonstrates that the symmetry of the order parameter is a non-universal property very sensitive to the microscopic details.

It is reasonable to ask if one can stabilize either of the remaining superconducting orders,  $\mathbf{d}^a$  or  $\Delta^s$ , by modification of the model's Hamiltonian. We can speculate that this might be possible provided that the spin-spin interaction is enhanced. Indeed, by examining Eq. (77) and Eq. (90) one concludes that  $\Delta^s$  ( $d_{x^2-y^2}$ -wave) could be non-zero if:

$$3\tilde{J}_{2k_F}^\perp > \tilde{g}_{2k_F}^\perp. \quad (92)$$

Such situation may be realized in a system with sufficiently large  $g_{bs}$  (to suppress CDW fluctuations) and sufficiently small bare values of  $g_{2k_F}^\perp$ .

As for  $\mathbf{d}^a$ , it is always zero: the constants in front of  $\mathbf{d}^a$  are strictly positive in both Eq.(77) and Eq.(90).

Thus, we demonstrate that the Q1D metal allows for a broad class of superconducting orders. The choice between these orders depends on both the band structure and the interaction constants.

### C. Other theoretical approaches

The root of the superconductivity in the real-life Q1D materials remains an unresolved issue. It is often suggested that the superconductivity in these compounds is not of phonon but rather of electron origin. There have been many attempts to construct a mechanism in line with this suggestion.

The theoretical literature on the subject can be split into two groups according to tools used. The studies employing the random phase approximation (RPA) or the fluctuation exchange approximation (FLEX) [7, 8, 9, 10] constitute the first group. The second group is made of the papers where RG [5, 11, 12, 13, 14] is employed.

We have mentioned that our method is closely related to the RG transformation. Clearly, it will be interesting to compare our conclusions with the conclusions of other researchers who use similar strategies.

In Ref.[5, 11, 12, 13, 14] the zero-temperature phase diagram of the Q1D metal was mapped with the help of a numerical implementation of the one-loop RG flow. The authors of the latter papers were found that, if the bare transverse interactions are zero or extremely small, the system undergoes a transition from the SDW phase

to the superconducting phase with the order parameter  $\Delta_{ij}^s$  ( $d_{x^2-y^2}$ -wave).

Furthermore, it was determined that, if the bare constants  $g_{2k_F}^\perp$  are sufficiently big, the transition is from the CDW phase into the superconducting phase with the  $f$ -wave order parameter  $\mathbf{d}_{ij}^s$ .

The results of these papers can be understood within the framework of our approach. In the limit where the only non-zero inter-chain term is the transverse hopping ( $t \neq 0$ , [11]), the RG flow generates both  $\tilde{g}_{2k_F}^\perp$  and  $\tilde{J}_{2k_F}^\perp$ . These constants satisfy the relation Eq.(92). The mechanism behind this is described in the previous subsection.

As we pointed out, when Eq.(92) is valid, the most stable order parameter is  $\Delta_{ij}^s$  ( $d_{x^2-y^2}$ -wave). Thus, our conclusions agrees with findings of Ref.[11].

The limit studied in [12, 13] is not compatible with our Eq.(15). In the latter reference it was assumed that the in-chain backscattering is of the order of the in-chain forward scattering. Thus, we cannot apply our approach straightforwardly, but certain qualitative conclusions may be reached.

When bare  $g_{2k_F}^\perp$  is large, the effective coupling  $\tilde{J}_{2k_F}^\perp$  is small, and the effective coupling  $\tilde{g}_{2k_F}^\perp$  is large. The ground state of the system with good nesting is CDW. The destruction of the CDW phase takes place when the nesting becomes sufficiently poor. Once the CDW is gone, we find ourselves in a familiar situation where the stable superconducting order parameter is either  $\mathbf{d}^s$  ( $f$ -wave) or  $\Delta^a$  ( $d_{xy}$ -wave), consistent with  $f$ -wave found in [12, 13].

If we lower  $g_{2k_F}^\perp$  sufficiently, the stability of SDW state may be restored [12, 13]. The in-chain backscattering suppresses  $\tilde{g}_{2k_F}^\perp$  and promotes  $\tilde{J}_{2k_F}^\perp$ , ultimately leading to inequality (92). In such a regime the most stable order parameter is  $\Delta_{ij}^s$  ( $d_{x^2-y^2}$ -wave), which agrees with [12, 13].

The above argumentation lends additional support to the notion that the mechanism proposed in this paper is not an artifact of the variational approximation. It is also a convenient feature of our method that it is analytical and the results of other approaches can be understood within its framework.

Besides RG several authors use RPA or FLEX to determine the superconducting properties in the anisotropic Fermi systems [7, 8, 9, 10]. These approximations resemble the classical BCS scheme in which the phonons are replaced by boson-like excitations of some other kind. In the quoted papers the excitations mediating the attractive interaction between the electrons are spin-density and charge-density fluctuations.

The frameworks laid out by the RPA and FLEX schemes are very appealing and intuitive. They both predict that under certain condition the Q1D metal is an unconventional superconductor. There is, however, a weak point: both methods are unable to account for the peculiarities specific for 1D electron liquid. Such weakness artificially narrows the region of the parameter space where the superconductivity is stable.

Finally, the author recently developed a canonical transformation approach for 1D electron systems [15, 16, 17]. This method may be viewed as a generalization of the one discussed in this paper. The application of the canonical transformation method to the Q1D systems is in progress.

#### D. Experiment vs. theory

The question remains if the model and the mechanism discussed above are of relevance to the Q1D superconductors, such as TMTSF and TMTTF [5]. Of course, the latter compounds have very complicated crystallographic structure: orthorhombic lattice, possibility of anion ordering, dimerization [6]. Yet, one can hope that these difficulties are not of paramount importance as far as the superconducting mechanism is concerned.

If this hope is justified should be assessed by the mechanism's ability to reproduce main features of the experimental data, at least qualitatively. We can look at the presented model with a good degree of optimism for it captures two most salient properties of the superconductivity in TMTSF/TMTTF.

The first of these two features is the common boundary shared by the superconducting and the SDW phases on the pressure-temperature phase diagram: the diagram of Fig.2 is similar to the high-pressure part of the 'universal' phase diagram of the TMTSF/TMTTF compounds [18].

The second is the non-trivial orbital structure of the order parameter in the Q1D superconductors. There are numerous pieces of evidence in favor of the order parameter with zeros on the Fermi surface [19, 20, 21, 22, 23]. (However, there is a thermal transport measurement [24] which contradicts to this picture.) The order parameters  $\mathbf{d}_{ij}^s$  and  $\Delta_{ij}^{s,a}$  are of this kind. Therefore, the predictions of our model is in qualitative agreement with the experiment.

#### E. Conclusions

We proposed the superconducting mechanism for the strongly anisotropic electron model without attractive interaction. We have shown that there is a region in the parameter space where the superconductivity is stable and shares a common boundary with SDW. The model supports two types of unconventional superconducting order parameter. Our mechanism may be relevant for the organic superconductors.

#### VII. ACKNOWLEDGEMENTS

The author is grateful for the support provided by the Dynasty Foundation and by the RFBR grants No. 06-02-16691 and 06-02-91200.

- 
- [1] A.O. Gogolin, A.A. Nersesyan, A.M. Tsvelik, *Bosonization and Strongly Correlated Systems*, (Cambridge University Press, Cambridge, England, 1998).
- [2] A.V. Rozhkov, *Phys. Rev. B*, **68**, 115108 (2003).
- [3] C. Bourbonnais and L.G. Caron, *Europhys. Lett.*, **5**, 209 (1988).
- [4] Yasumasa Hasegawa and Hidetoshi Fukuyama, *J. Phys. Soc. Jpn.*, **55**, 3978 (1986).
- [5] N. Dupuis, C. Bourbonnais and J.C. Nickel, *Low Temp. Phys.*, **32**, 380 (2006).
- [6] T.Ishiguro, K. Yamaji, and G. Saito, *Organic Superconductors*, (Springer, Berlin, Germany, 1998).
- [7] Y.Tanaka and K. Kuroki, *Phys. Rev. B*, **70**, 060502(R) (2004).
- [8] Kazuhiko Kuroki and Yukio Tanaka, *J. Phys. Soc. Jpn.*, **74**, 1694 (2005).
- [9] Kazuhiko Kuroki, Ryotaro Arita, and Hideo Aoki, *Phys. Rev. B*, **63**, 094509 (2001).
- [10] Kazuhiko Kuroki, *J. Phys. Soc. Jpn.*, **75**, 051013 (2006).
- [11] Raphael Duprat, C. Bourbonnais, *Eur. Phys. J. B*, **21**, 219 (2001).
- [12] J.C. Nickel, R. Duprat, C. Bourbonnais, and N. Dupuis, *Phys. Rev. Lett.*, **95**, 247001 (2005) and *cond-mat/0502614*, v.2.
- [13] J. C. Nickel, R. Duprat, C. Bourbonnais, and N. Dupuis, *Phys. Rev. B*, **73**, 165126 (2006).
- [14] C. Bourbonnais, preprint *cond-mat/0204345*.
- [15] A.V. Rozhkov, *Eur. Phys. J. B*, **47**, 193 (2005).
- [16] A.V. Rozhkov, *Phys. Rev. B*, **74**, 245123 (2006).
- [17] A.V. Rozhkov, *Phys. Rev. B*, **77**, 125109 (2008).
- [18] H. Wilhelm, D. Jaccard, R. Duprat, C. Bourbonnais, D. Jerome, J. Moser, C. Carcel, and J. M. Fabre, *Eur. Phys. J. B*, **21**, 175 (2001).
- [19] I.J. Lee, S.E. Brown, W.G. Clark, M.J. Strouse, M.J. Naughton, W. Kang, and P.M. Chaikin, *Phys. Rev. Lett.*, **88**, 017004 (2001).
- [20] I.J. Lee, D.S. Chow, W.G. Clark, M.J. Strouse, M.J. Naughton, P.M. Chaikin, and S.E. Brown, *Phys. Rev. B*, **68**, 092510 (2003).
- [21] N. Joo, P. Auban-Senzier, C.R. Pasquier, P. Monod, D. Jérôme, and K. Bechgaard, *Eur. Phys. J. B*, **40**, 43 (2004).
- [22] I.J. Lee and M.J. Naughton, G.M. Danner and P.M. Chaikin, *Phys. Rev. Lett.*, **78**, 3555 (1997).
- [23] J.I. Oh and M.J. Naughton, *Phys. Rev. Lett.*, **92**, 067001, (2004).
- [24] Stéphane Belin and Kamran Behnia, *Phys. Rev. Lett.*, **79**, 2125 (1997).

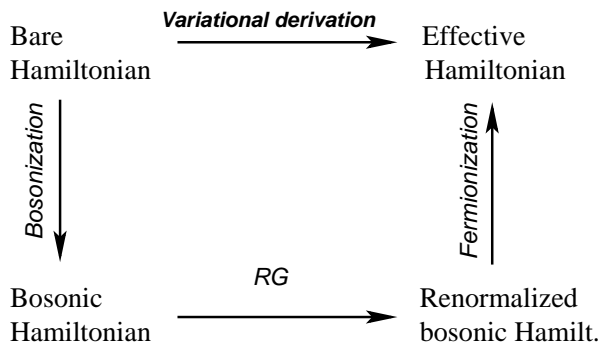


FIG. 1: The relation between the variation procedure and the tree-level RG.

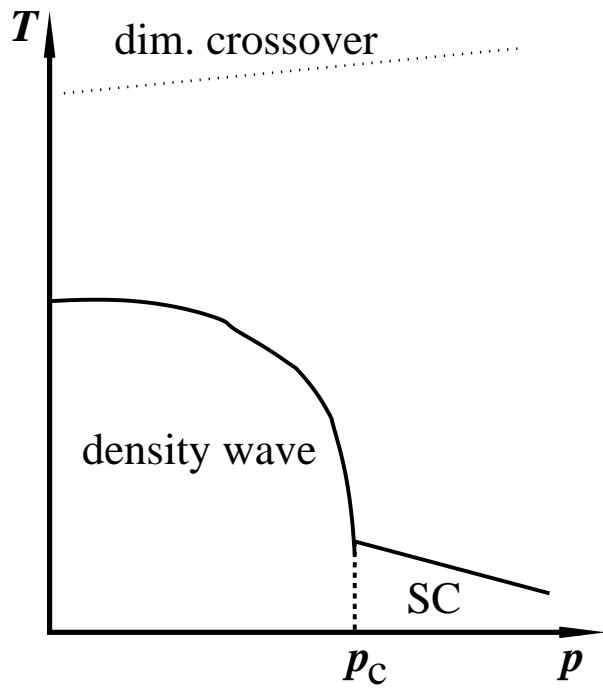


FIG. 2: Qualitative phase diagram of our model. Solid lines show second-order phase transitions into density wave and the superconducting phases. Dashed line shows the first-order transition between these phases. The dotted line at high temperature shows location of the dimensional crossover.